Published in final edited form as:
Mol Genet Metab. 2004 April ; 81(Suppl 1): S4–11. doi:10.1016/j.ymgme.2003.10.017.

Mammalian N-acetylglutamate synthase

Hiroki Morizono, **Ljubica Caldovic**, **Dashuang Shi**, and **Mendel Tuchman***
Children's Research Institute, Children's National Medical Center, The George Washington University, 111 Michigan Ave NW, Washington, DC 20010, USA

Abstract

N-Acetylglutamate synthase (NAGS, E.C. 2.3.1.1) is a mitochondrial enzyme that catalyzes the formation of *N*-acetylglutamate (NAG), an essential allosteric activator of carbamylphosphate synthetase I (CPSI). The mouse and human NAGS genes have been identified based on similarity to regions of NAGS from *Neurospora crassa* and cloned from liver cDNA libraries. These genes were shown to complement an argA-(NAGS) deficient *Escherichia coli* strain, and enzymatic activity of the proteins was confirmed by a new stable isotope dilution assay. The deduced amino acid sequence of mammalian NAGS contains a putative mitochondrial-targeting signal at the N-terminus. The mouse NAGS preprotein was overexpressed in insect cells to determine post-translational modifications and two processed proteins with different N-terminal truncations have been identified. Sequence analysis using a hidden Markov model suggests that the vertebrate NAGS protein contains domains with a carbamate kinase fold and an acyl-CoA *N*-acyltransferase fold, and protein crystallization experiments are currently underway. Inherited NAGS deficiency results in hyperammonemia, presumably due to the loss of CPSI activity. We, and others, have recently identified mutations in families with neonatal and late-onset NAGS deficiency and the identification of the gene has now made carrier testing and prenatal diagnosis feasible. A structural analog of NAG, carbamylglutamate, has been shown to bind and activate CPSI, and several patients have been reported to respond favorably to this drug (Carbaglu®).

Introduction

N-Acetylglutamate (NAG) is an obligatory allosteric activator of carbamylphosphate synthase I (CPSI) and is produced in the mitochondrial matrix from glutamate and acetyl coenzyme-A by *N*-acetylglutamate synthase (NAGS) [1-3]. NAGS is expressed primarily in liver and small intestine and may have a key role as a regulator of ureagenesis by modulating the activity of CPSI through NAG [4,5]. Inherited NAGS deficiency appears to cause hyperammonemia due to secondary deficiency of CPSI deprived of its cofactor NAG [6].

NAGS has been purified to apparent homogeneity from human and rat liver [7-9]. The enzyme appears to be a trimer but forms higher order oligomers upon the addition of L-arginine [8]. In contrast to NAGS of bacteria and fungi which is inhibited by arginine, mammalian NAGS activity increases three to fivefold in the presence of arginine [9-11]. NAGS activity is also stimulated by protamines and other cationic polypeptides (e.g., polyarginine and polylysine) [9].

We have recently identified and cloned both the mouse and human NAGS genes, and found several deleterious mutations in patients. A rapid and specific stable isotope LC–MS method

*Corresponding author. Fax: 1-202-884-6014. mtuchman@cnmc.org (M. Tuchman)..

for measuring NAG has also been developed to quantify NAGS activity [12-15], which has been used in the studies described herein.

Identification and cloning of the first mammalian NAGS gene

One of the confounding factors in cloning any vertebrate NAGS was that unlike the other urea cycle enzymes, NAGS has a low degree of sequence conservation across phyla [16]. The human NAGS gene sequence was initially identified using the *Neurospora crassa* NAGS (Arg-14) protein sequence to probe the human genome using tblastn [17]. A short region of similarity containing approximately 130 amino acids was identified on chromosome 17, band 17q21.31. Use of *Saccharomyces pombe* NAGS as a query identified the same region but with an *E* value of only 0.006, while querying with *Saccharomyces cerevisiae* NAGS did not return any significant candidates using the same EXPECT threshold. Alignment of the three fungal NAGS protein sequences with each other using GCG PILEUP with the default gap and gap length weights (8 and 2, respectively), resulted in 48 identical amino acids in the region of the human sequence identified by BLAST. Of these identical amino acids, 25 were also conserved in the BLAST pairwise alignment between the *N. crassa* and the human sequence. The human sequence was then used to query the mouse genome, and the homologous sequence was identified within the syntenic region on chromosome 11. Gene models for both the mouse and human candidates were constructed using GRAIL, and were used to query mouse and human EST libraries to obtain an open reading frame. Pairwise alignments between the mouse and *N. crassa* NAGS sequences using GCG GAP with defaults weights showed the two sequences to share 33% similarity overall, but alignment of the mouse sequence to the *N. crassa N*-acetylglutamate kinase sequence also had a 32% similarity. To assign the identity of the gene, candidate sequences constructed by overlapping several ESTs for mouse and human NAGS were cloned into pUC-based expression vectors. These were shown to complement argA-(NAGS) deficient arginine auxotrophic strains of *Escherichia coli*, confirming that the genes did indeed encode proteins able to synthesize NAG [14]. Systematic querying of the GenBank databases and other genome projects has yielded, to date, three additional vertebral NAGS candidates (zebrafish, fugu, and rat). Northern analysis was performed to determine the tissue distribution of the NAGS message. NAGS is primarily expressed in liver and small intestine, tissues in which CPSI is also exclusively expressed. Interestingly, a low level of expression is also detectable in kidney, testis, and spleen which could indicate other roles for NAGS beyond providing an essential cofactor for CPSI [12,14].

Protein sequence

Human NAGS is synthesized as a preprotein of 534 amino acids [12]. Because the enzyme is localized to the mitochondria, it was assumed that the N-terminal portion contains a targeting peptide that is subsequently cleaved. Two possible signal peptide cleavage sites were predicted after positions 31 and 49 using rules described by Ito [18] and Neupert [19]. These were dubbed the amino termini of the “long mature” and “short mature” protein, respectively. Alignment of mouse and human NAGS protein sequences (Fig. 1) shows an interesting bipartite pattern within the N-terminal region, with the first 49 amino acids having a composition consistent with a mitochondrial signal sequence (63% identity between mouse and human), and the next 45 amino acids dubbed the “variable domain” having relatively low homology (35% identity). The remaining 440 amino acids (“conserved domain”) share 92% identity. Additions of the piscine sequences to the alignment show a similar pattern, with a marked increase in homology beginning at the “conserved domain.”

As described above, initial analysis of the protein sequence revealed sequence similarity to both the *N*-acetylglutamate kinase and synthase of Neurospora. Using the Superfamily

server, a hidden Markov model-based protein fold library, the domain architecture of the vertebrate NAGS protein is predicted to have a carbamate kinase-like fold for amino acids 137–373 and an acyl-CoA *N*-acyltransferase-like fold for residues 377–472 [20,21]. Carbamate kinase has structural similarities to *E. coli N*-acetylglutamate kinase, suggesting that the region 137–373 contains the glutamate binding domain, while region 377–472 is part of the acetyl-CoA binding domain. The adenine nucleotide moiety of acetyl-CoA may also be recognized by region 137–373. The crystal structures of *E. coli N*-acetylglutamate kinase (NAGK) complexed with NAG and AMP (1GS5) and the histone acetyltransferase domain of P300/CBP Associating Factor (PCAF) containing CoA (1CM0) were examined, and 57 active site residues involved in binding CoA, NAG, or AMP were identified using the LPC server [22-24]. The sequences of human NAGS and these proteins were separately aligned to the hidden Markov models for the carbamate kinase-like fold and for the acyl-CoA *N*-acyltransferase fold. Corresponding regions were examined to determine if active site residues in the NAGS sequence might be revealed by combining this information with sequence conservation between the vertebrate NAGS proteins, assuming that residues conserved among the NAGS species are most likely to be important for proper folding and function. The overall conservation is low as would be expected from a comparison of such disparate sequences, but based on this analysis, it appears that the CoA binding site can be predicted to reside within two conserved islands of amino acids 415–450 and 465–485. Residues involved in binding NAG in the NAGK structure occur at regions of insertions and deletions in the alignment, making it less likely that the Superfamily alignment generated for NAGK and NAGS is able to correctly identify NAG binding residues in NAGS (Fig. 2).

Development of an LC–MS based enzyme assay

To better characterize the function of recombinant NAGS, we developed a simple, rapid and accurate method for assaying NAGS enzymatic activity that does not require radioisotopic compounds. To this end, a GC–MS stable isotope dilution approach had been previously developed in the lab, but this method requires prior column separation, making it less suitable for large-scale kinetic experiments [25]. We adapted instead a stable isotope dilution method using liquid chromatography mass spectrometry (LC–MS) to measure NAG production. Enzymatic activity is assayed in 50 mM Tris buffer, pH 8.5, containing 10 mM glutamate and 2.5 mM acetyl-CoA in a 100 μl reaction volume. Where applicable, 1 mM L-arginine is added to the assay mixture. The reaction is initiated by the addition of enzyme, and the mixture is incubated at 30 °C for 5 min. The reaction is quenched with 30% trichloroacetic acid containing 50 μg of *N*-acetyl-[$^{13}C_5$]glutamate (^{13}C-NAG, internal standard). The precipitated protein is removed by micro-centrifugation for 5 min.

Glutamate, NAG, and ^{13}C-NAG are readily separated on reverse phase HPLC; the mobile phase consists of 93% solvent A (1 ml trifluoroacetic acid in 1 L water) and 7% solvent B (1 ml trifluoroacetic acid in 1 L of 1:9 water/acetonitrile). The flow rate is 0.6 ml/min. Glutamate, NAG, and ^{13}C-NAG are detected and quantified by selected ion monitoring mass spectrometry. Changing the mobile phase to 100% solvent A increases the separation between glutamate and NAG, also making possible the separation of *N*-carbamylglutamate. NAGS reaction chromatograms are shown in Fig. 3. The LC–MS assay in its current form is capable of detecting enzyme activity from an open biopsy sample starting with approximately 30–100 mg of liver tissue, and is in the process of being enhanced for use with sample amounts commonly obtained from a needle biopsy.

Enzyme characterization

Enzyme assays performed with the preprotein, “short mature,” “long mature,” and “conserved domain” versions of NAGS show that the enzyme is active in all three forms, and remains arginine-responsive in all.

Human and mouse recombinant NAGS bearing polyhistidine tags were overexpressed in *E. coli* and purified using nickel affinity chromatography. Enzymatic activity was measured for four variants of mouse NAGS: preprotein, two versions of the putative “mature” protein (long and short) and the conserved domain. “Short mature” NAGS had the highest specific activity. The conserved domain of human and mouse NAGS had lower specific activity suggesting that the variable domain either enhances catalytic activity or stabilizes the NAGS protein. Enzymatic activities of recombinant proteins increased two to sixfold in the presence of 1 mM arginine [12,14].

Post-translational processing

To determine if and where mitochondrial processing occurs, the mouse NAGS preprotein fused to a C-terminal polyhistidine tag was overexpressed in insect cells using a baculovirus system, and the resulting protein was purified under native conditions with an immobilized nickel affinity column. Three strong bands were seen when the affinity-purified samples were run on SDS–PAGE followed by Coomassie staining. These bands were excised, and subjected to rapid, in-gel, trypsin digestion [26]. The isolated fragments were analyzed using mass spectrometry on an Applied Biosystems Voyager 4700 MALDI TOF/TOF. All three samples contained a characteristic peak with an *m/z* of 1150. This peak from each of the samples was sequenced using collision-induced dissociation and found to correspond to the internal peptide LAFALAFLQR of NAGS (Fig. 4). The same sample was separated on SDS–PAGE, blotted onto Immobilon-P^{SQ}, and then stained with Coomassie blue. Bands corresponding to the two shorter proteins were submitted for amino acid sequencing at the Texas A&M Laboratory for Protein Chemistry. These two smaller bands yielded a cleavage site of the canonical mitochondrial leader peptide to be after amino acid 50 and revealed a second cleavage site at the end of the variable domain after amino acid 91. There are several precedents for bipartite signaling peptides; ornithine transcarbamylase is imported into the mitochondria in a two-stage cleavage process [27]. In other mitochondrial proteins such as cytochrome *b*2 and cytochrome *c*1, bipartite signaling peptides containing a hydrophobic stretch are thought to be a suborganellar sorting signal [28,29]. Unlike the bipartite signal seen in the cytochrome proteins, the variable domain is not particularly hydrophobic, suggesting a different role for this region of NAGS.

NAGS deficiency

Several reports of NAGS deficiency exist in the literature; however, definitive diagnosis was unavailable until the gene sequence became available. Owing to a lack of specific biochemical markers, and the low abundance of NAGS, currently not amenable to assay from needle liver biopsies, it is likely that NAGS deficiency is under-diagnosed. Deficiency of NAG can be caused either by genetic defects of NAGS or by secondary effects of certain organic acid disorders, fatty acid oxidation defects, and by the administration of valproic acid; the secondary effects appear to be due to inhibition of NAGS by metabolites that contain CoA [30]. The symptoms of inherited NAGS deficiency appear very similar to CPSI deficiency, with elevated plasma ammonia and glutamine, reduced or absent citrulline, and normal urinary orotate. As expected, when CPSI enzyme assays supplemented with NAG are performed on liver biopsies from NAGS-deficient patients normal CPS activity is seen. Table 1 summarizes mutations identified in 10 families with NAGS deficiency. A variable reduction in NAGS activity and/or arginine activation has been observed, with some patients

showing normal activity. However, there are some concerns about the reliability of the activity assay; a patient reported to have normal basal enzyme activity was shown through subsequent mutation analysis to have a null frameshift mutation [31]. It is possible that other acylases in liver homogenates are also capable of catalyzing the transfer of an acetyl group onto glutamate, making further development of the assay necessary. Normal NAGS activity has been reported to be >34 nmol/min/g tissue, and upon arginine stimulation increases to >144 nmol/min g tissue [25].

Other mutations

Although only a few NAGS mutations have been identified in patients to date, some predictions can be made of regions likely to prove important for structure and function. In sequence alignments of ornithine transcarbamylase, the conservation of amino acid properties across species has been successfully applied to evaluate amino acid loci that result in “neonatal” vs. “late-onset” hyperammonemia, and to identify regions of the protein involved in substrate binding and catalysis [32]. Alignment of the mouse and human NAGS amino acid sequences clearly identifies several well-conserved motifs. The addition of piscine sequences helps further refine these motifs by providing additional genetic “distance.” In the current alignment, 197 amino acids are identical across vertebral species. Deleterious mutations of NAGS have been identified in patients corresponding to these regions of strong conservation [13,31,33].

In the course of generating sufficient protein for structural studies of NAGS, aggregation of the protein was discovered to be a significant challenge. The structural rationale is that unfavorable protein–protein interactions are promoting aggregation. Attempts to engineer a more soluble NAGS through random PCR mutagenesis combined with DNA shuffling have an additional benefit of making it possible to observe many more deleterious mutations in the NAGS gene. Several candidate proteins were isolated with increased solubility compared to wild type, and upon DNA sequencing each was found to have multiple mutations. In this experiment, there is no selection pressure to maintain enzyme activity, but with the exception of those proteins containing mutations in strongly conserved amino acids, the others retained enzymatic activity. The possibility remains that compensating mutations occur that together preserve activity, despite individually being deleterious. Still, this type of DNA shuffling experiment may have general utility as a way to rapidly extract information about change-tolerant regions in proteins whose structures are yet unsolved. These regions are also likely to be polymorphic sites in patients rather than strongly deleterious, and several mutations can be mapped from each experiment.

Treatment

With the availability of the NAGS sequence, deficiencies in the gene can now be reliably confirmed, providing a tool for carrier testing and prenatal diagnosis that was not previously available [13]. Moreover, a specific treatment for NAGS deficiency using *N*-carbamylglutamate, a NAG structural analog, to activate CPSI is available and approved for use in Europe (Carbaglu®, Orphan Europe). Several reports have shown that carbamylglutamate is apparently effective in the treatment of NAGS deficiency [31,33-38]. With the availability of molecular diagnosis, early confirmation of NAGS deficiency becomes particularly compelling, as treatment with *N*-carbamylglutamate may be effective in preventing hyperammonemia and brain damage.

Conclusions

NAGS produces a unique, and the only known, enzymatic cofactor for the urea cycle. There is evidence that the availability of this cofactor may modulate the activity of CPSI and

hence, the flux through the urea cycle. Understanding NAGS deficiency can help perhaps to better understand the regulation of ureagenesis, while the availability of a stable analog of NAG may provide the first specific treatment of a severe urea cycle disorder.

Acknowledgments

We thank Maria Panglao for technical assistance, Mark Williams of the University of Minnesota Recombinant Protein Expression Laboratory for preparing baculovirus infected cell pastes, and Larry Dangott of the Texas A&M University Laboratory for Protein Chemistry, for N-terminal sequencing of the NAGS variants. This work was supported by public health service Grants R01DK47870 and R01DK064913 from the National Institute of Diabetes Digestive and Kidney Diseases and Grant P30HD040677 from the National Center for Child Health and Human Development and Grant M01-RR13297 from the General Clinical Research Center Program of the National Center for Research Resources, National Institutes of Health, Department of Health and Human Services.

References

[1]. Grisolia S, Cohen PP. Catalytic role of glutamate derivatives in citrulline biosynthesis. J. Biol. Chem 1953;204:753–757. [PubMed: 13117851]

[2]. Marshall M, Metzenberg RL, Cohen PP. Purification of carbamyl phosphate synthetase from frog liver. J. Biol. Chem 1958;233:102–105. [PubMed: 13563449]

[3]. Shigesada K, Tatibana M. Enzymatic synthesis of acetylglutamate by mammalian liver preparations and its stimulation by arginine. Biochem. Biophys. Res. Commun 1971;44:1117–1124. [PubMed: 5160402]

[4]. Meijer AJ, Lof C, Ramos IC, Verhoeven AJ. Control of ureagenesis. Eur. J. Biochem 1985;148:189–196. [PubMed: 3979393]

[5]. Tujioka K, Lyou KS, Hirano E, Sano A, Hayase K, Yoshida A, Yokogoshi H. Role of *N*-acetylglutamate concentration and ornithine transport into mitochondria in urea synthesis of rats given proteins of different quality. J. Agric. Food Chem 2002;50:7467–7471. [PubMed: 12452677]

[6]. Bachmann C, Colombo JP, Jaggi K. *N*-Acetylglutamate synthetase (NAGS) deficiency: diagnosis, clinical observations and treatment. Adv. Exp. Med. Biol 1982;153:39–45. [PubMed: 7164912]

[7]. Bachmann C, Krahenbuhl S, Colombo JP. Purification and properties of acetyl-CoA: l-glutamate *N*-acetyltransferase from human liver. Biochem. J 1982;205:123–127. [PubMed: 7126172]

[8]. Shigesada K, Tatibana M. *N*-Acetylglutamate synthetase from rat-liver mitochondria. Partial purification and catalytic properties. Eur. J. Biochem 1978;84:285–291. [PubMed: 25771]

[9]. Sonoda T, Tatibana M. Purification of *N*-acetyl-l-glutamate synthetase from rat liver mitochondria and substrate and activator specificity of the enzyme. J. Biol. Chem 1983;258:9839–9844. [PubMed: 6885773]

[10]. Cybis J, Davis RH. Organization and control in the arginine biosynthetic pathway of *Neurospora*. J. Bacteriol 1975;123:196–202. [PubMed: 166979]

[11]. Jauniaux JC, Urrestarazu LA, Wiame JM. Arginine metabolism in *Saccharomyces cerevisiae*: subcellular localization of the enzymes. J. Bacteriol 1978;133:1096–1107. [PubMed: 205532]

[12]. Caldovic L, Morizono H, Gracia Panglao M, Gallegos R, Yu X, Shi D, Malamy MH, Allewell NM, Tuchman M. Cloning and expression of the human *N*-acetylglutamate synthase gene. Biochem. Biophys. Res. Commun 2002;299:581–586. [PubMed: 12459178]

[13]. Caldovic L, Morizono H, Panglao MG, Cheng SF, Packman S, Tuchman M. Null mutations in the *N*-acetylglutamate synthase gene associated with acute neonatal disease and hyperammonemia. Hum. Genet 2003;112:364–368. [PubMed: 12594532]

[14]. Caldovic L, Morizono H, Yu X, Thompson M, Shi D, Gallegos R, Allewell NM, Malamy MH, Tuchman M. Identification, cloning and expression of the mouse *N*-acetylglutamate synthase gene. Biochem. J 2002;364:825–831. [PubMed: 12049647]

[15]. Caldovic L, Tuchman M. *N*-Acetylglutamate and its changing role through evolution. Biochem. J 2003;372:279–290. [PubMed: 12633501]

[16]. Yu YG, Turner GE, Weiss RL. Acetylglutamate synthase from *Neurospora crassa*: structure and regulation of expression. Mol. Microbiol 1996;22:545–554. [PubMed: 8939437]

[17]. Altschul SF, Gish W, Miller W, Myers EW, Lipman DJ. Basic local alignment search tool. J. Mol. Biol 1990;215:403–410. [PubMed: 2231712]

[18]. Ito A. Mitochondrial processing peptidase: multiple-site recognition of precursor proteins. Biochem. Biophys. Res. Commun 1999;265:611–616. [PubMed: 10600469]

[19]. Neupert W. Protein import into mitochondria. Annu. Rev. Biochem 1997;66:863–917. [PubMed: 9242927]

[20]. Gough J, Karplus K, Hughey R, Chothia C. Assignment of homology to genome sequences using a library of hidden Markov models that represent all proteins of known structure. J. Mol. Biol 2001;313:903–919. [PubMed: 11697912]

[21]. Hubbard TJ, Murzin AG, Brenner SE, Chothia C. SCOP: a structural classification of proteins database. Nucleic Acids Res 1997;25:236–239. [PubMed: 9016544]

[22]. Ramon-Maiques S, Marina A, Gil-Ortiz F, Fita I, Rubio V. Structure of acetylglutamate kinase, a key enzyme for arginine biosynthesis and a prototype for the amino acid kinase enzyme family, during catalysis. Structure 2002;10:329–342. [PubMed: 12005432]

[23]. Clements A, Rojas JR, Trievel RC, Wang L, Berger SL, Marmorstein R. Crystal structure of the histone acetyltransferase domain of the human PCAF transcriptional regulator bound to coenzyme A. EMBO J 1999;18:3521–3532. [PubMed: 10393169]

[24]. Sobolev V, Sorokine A, Prilusky J, Abola EE, Edelman M. Automated analysis of interatomic contacts in proteins. Bioinformatics 1999;15:327–332. [PubMed: 10320401]

[25]. Tuchman M, Holzknecht RA. Human hepatic *N*-acetylglutamate content and *N*-acetylglutamate synthase activity. Determination by stable isotope dilution. Biochem. J 1990;271:325–329. [PubMed: 2241918]

[26]. Havlis J, Thomas H, Sebela M, Shevchenko A. Fast-response proteomics by accelerated in-gel digestion of proteins. Anal. Chem 2003;75:1300–1306. [PubMed: 12659189]

[27]. Sztul ES, Hendrick JP, Kraus JP, Wall D, Kalousek F, Rosenberg LE. Import of rat ornithine transcarbamylase precursor into mitochondria: two-step processing of the leader peptide. J. Cell Biol 1987;105:2631–2639. [PubMed: 3693395]

[28]. Hartl FU, Ostermann J, Guiard B, Neupert W. Successive translocation into and out of the mitochondrial matrix: targeting of proteins to the intermembrane space by a bipartite signal peptide. Cell 1987;51:1027–1037. [PubMed: 2826012]

[29]. Nicholson DW, Stuart RA, Neupert W. Biogenesis of cytochrome *c*1. Role of cytochrome *c*1 heme lyase and of the two proteolytic processing steps during import into mitochondria. J. Biol. Chem 1989;264:10156–10168. [PubMed: 2542325]

[30]. Coude FX, Sweetman L, Nyhan WL. Inhibition by propionylcoenzyme A of *N*-acetylglutamate synthetase in rat liver mitochondria. A possible explanation for hyperammonemia in propionic and methylmalonic acidemia. J. Clin. Invest 1979;64:1544–1551. [PubMed: 500823]

[31]. Elpeleg O, Shaag A, Ben-Shalom E, Schmid T, Bachmann C. *N*-Acetylglutamate synthase deficiency and the treatment of hyperammonemic encephalopathy. Ann. Neurol 2002;52:845–849. [PubMed: 12447942]

[32]. Tuchman M, Morizono H, Reish O, Yuan X, Allewell NM. The molecular basis of ornithine transcarbamylase deficiency: modelling the human enzyme and the effects of mutations. J. Med. Genet 1995;32:680–688. [PubMed: 8544185]

[33]. Haberle J, Schmidt E, Pauli S, Kreuder JG, Plecko B, Galler A, Wermuth B, Harms E, Koch HG. Mutation analysis in patients with *N*-acetylglutamate synthase deficiency. Hum. Mutat 2003;21:593–597. [PubMed: 12754705]

[34]. Grau E, Felipo V, Minana MD, Grisolia S. Treatment of hyperammonemia with carbamylglutamate in rats. Hepatology 1992;15:446–448. [PubMed: 1544625]

[35]. Guffon N, Vianey-Saban C, Bourgeois J, Rabier D, Colombo JP, Guibaud P. A new neonatal case of *N*-acetylglutamate synthase deficiency treated by carbamylglutamate. J. Inherit. Metab. Dis 1995;18:61–65. [PubMed: 7623444]

[36]. Hinnie J, Colombo JP, Wermuth B, Dryburgh FJ. *N*-Acetylglutamate synthetase deficiency responding to carbamylglutamate. J. Inherit. Metab. Dis 1997;20:839–840. [PubMed: 9427158]

[37]. Morris AA, Richmond SW, Oddie SJ, Pourfarzam M, Worthington V, Leonard JV. *N*-Acetylglutamate synthetase deficiency: favourable experience with carbamylglutamate. J. Inherit. Metab. Dis 1998;21:867–868. [PubMed: 9870213]

[38]. Schubiger G, Bachmann C, Barben P, Colombo JP, Tonz O, Schupbach D. *N*-Acetylglutamate synthetase deficiency: diagnosis, management and follow-up of a rare disorder of ammonia detoxification. Eur. J. Pediatr 1991;150:353–356. [PubMed: 2044610]

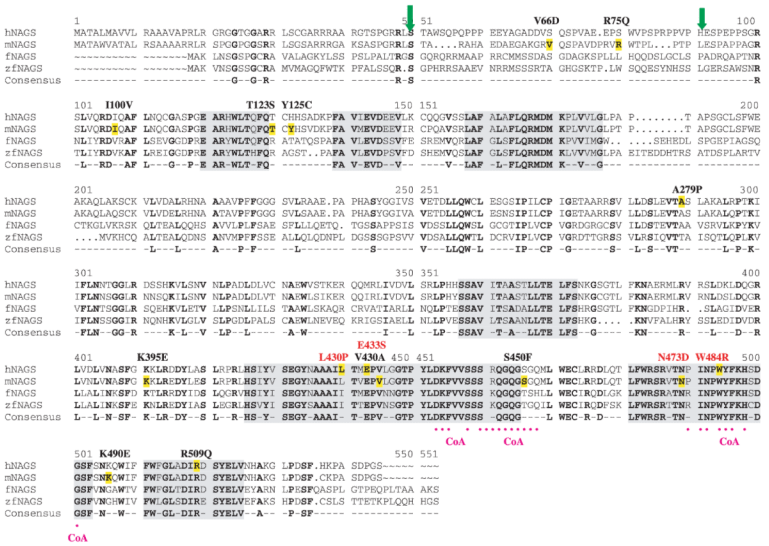

Fig. 1.

Alignment of vertebrate NAGS proteins. Legend: hNAGS, human; mNAGS, mouse; fNAGS, fugu; and zfNAGS, zebrafish. Missense mutations found in patients or those generated by random mutagenesis in the mouse sequence are marked in yellow, and the resulting amino acid change is labeled above the alignment. Mutations known to be deleterious are shown in red. Strongly conserved blocks are shaded in gray. Residues predicted to be active site residues are marked with dots below the alignment. Arrows at position 51 and 92 indicate the start sites of the two processed NAGS proteins dubbed “short mature” and “conserved domain.” Discrepancies between mutation numbering and alignment position number are due to insertions when generating the alignment.

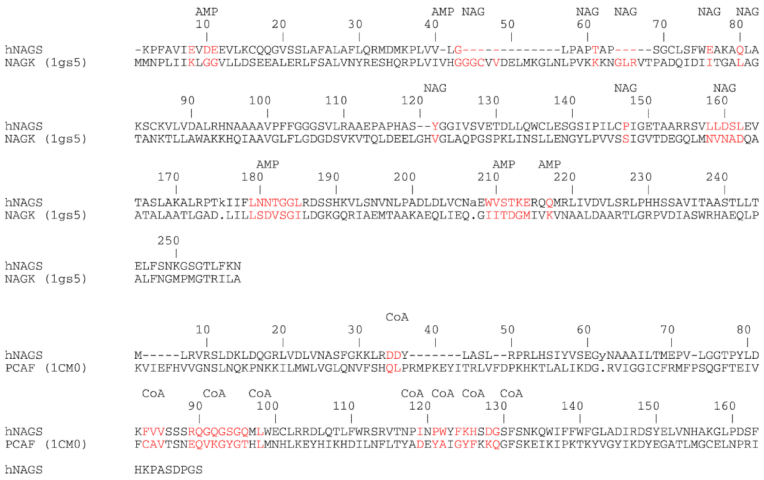

Fig. 2.

Hidden Markov model based alignment of human NAGS sequence with *E. coli N*-acetylglutamate kinase (NAGK) and with the histone acetyltransferase domain of P300/CBP associating factor (PCAF). Active site residues determined from the crystal structures of NAGK and PCAF are highlighted in red, along with their counterparts in the NAGS sequence. The alignment between hNAGS and NAGK has several shortcomings, including long insertions in the region of active site residues and relatively poor conservation of active site residues. This argues that the alignment cannot be used to correctly identify the NAG binding residues within NAGS.

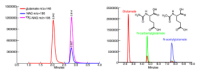

Fig. 3.

Liquid chromatography–mass spectrometry based NAGS enzyme assay. Left panel: typical stable isotope dilution sample. The ratio between a known amount of isotopic NAG and the NAG produced in the assay is used to quantitate NAG formation. Right panel: separation conditions can be modified to simultaneously monitor glutamate, carbamylglutamate, and NAG. Peaks corresponding to glutamate, *N*-acetylglutamate, and *N*-carbamylglutamate are shown with the chemical structures of *N*-carbamylglutamate and *N*-acetylglutamate.

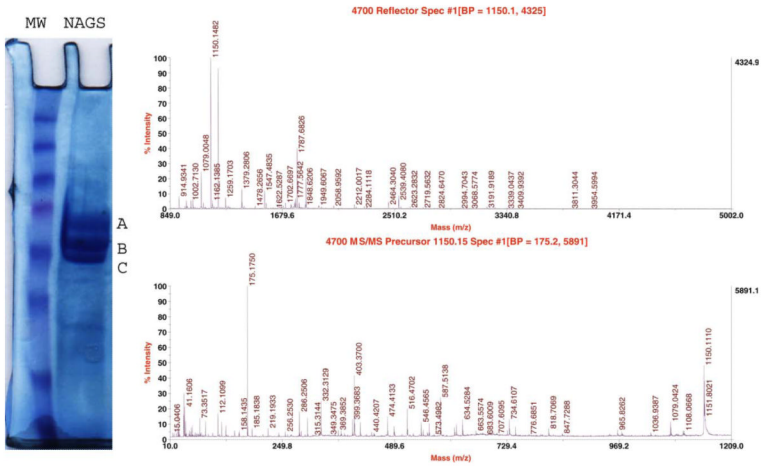

Fig. 4.

Identification of processing sites in NAGS. (Left) SDS–PAGE of nickel affinity purified NAGS expressed in insect cells. Three major isoforms are visible corresponding to preprotein (A), “short mature” (B), and “conserved domain” (C). (Right) MS spectra and MS/MS spectra following in gel tryptic digestion of the uppermost band. All three bands contain a characteristic 1150 *m/z* peak in their tryptic MS spectra that corresponds to the peptide LAFALAFLQR of NAGS upon analysis using MS/MS mode.

Table 1

Known mutations in the human NAGS gene

Patient/family	Ethnic origin	Nucleotide change	Mutation type	Enzyme activity basal/with Arg	Phenotype	Ref.
1	Caucasian	TGG→TAG	Trp324Ter	10/20	Neonatal	Caldovic et al. [13]
2	Latino	1025delG	Frameshift	nd	Neonatal	
3	Caucasian	CGG→CAG/ INS4-1G>C	Arg509Gln/ac-ceptor splice site	nd	Late onset	Unpublished
4	Iranian Jewish	1036insC	Frameshift	141/74	Neonatal	Elpeleg et al. [31]
5	German	1036insT/ IVS3-2A>T	Frameshift/ac-ceptor splice site	6/14	Neonatal	Haberle et al. [33]
6	Slovenian	GCG→ACG	Ala279Pro	22/22	Late onset	
7	Turkish	CTG→CCG	Leu430Pro	14/19	Neonatal	
8	Turkish	TGG→TAG	Trp324Ter	nd	Neonatal	
9	Turkish	TGG→CGG	Trp484Arg	nd	Neonatal	
10	German	GAG→CAG	Glu433Ser	0/72	Neonalat	

Nucleotide and codon numbering is from the translation start site.